

Large-Signal Behavioral Modeling of Nonlinear Amplifiers Based on Load–Pull AM–AM and AM–PM Measurements

Jiang Liu, Lawrence P. Dunleavy, *Senior Member, IEEE*, and Huseyin Arslan, *Senior Member, IEEE*

Abstract—This paper presents an improved behavioral modeling technique that generates large-signal models for nonlinear amplifiers or devices based on load–pull AM–AM and AM–PM measurement datasets. The generated behavioral model characterizes the incident and scattering waveforms at two ports in the frequency domain based on the large-signal scattering function theory. The advantage of this technique is that it is derived entirely from load–pull measurements and provides an analytic method to utilize the load–pull measurements in practical designs. Examples are given to demonstrate the ability of the behavioral models to predict the load-related nonlinearities of the device-under-test.

Index Terms—Large signal, microwave measurements, modeling, network analysis, nonlinear systems, scattering parameters.

I. INTRODUCTION

BEHAVIORAL modeling of RF components is receiving more and more interest recently. This is because of the increasing application of integrated circuits in wireless products, e.g., cellular phones and personal digital assistants (PDAs). Accurate behavioral models for these off-the-shelf components are very important for this practice to be successful. Probably the most successful behavioral model is the small-signal scattering parameter set that characterizes linear and mildly nonlinear devices and components. S -parameter representation is a frequency-domain behavioral model for the network studied, characterizing the relationship between the incident and scattering waveforms at specific frequencies, one at a time. Since it deals with linear transfer relationship only, it cannot be used to model components [e.g., power amplifiers (PAs)] that present significant nonlinearities. However, with the advance of modern wireless communication systems, more and more demands are generated for nonlinear operation of devices and amplifiers to get better transmission efficiency and less power consumption.

A large-signal scattering function theory is proposed to augment the limitation of the small-signal S -parameter representation. This theory, which has been extensively studied, e.g., [1]–[6], extends small-signal theory to take into account not only the fundamental, but also harmonics at different ports. The contribution of all these spectral components is formulated into nonlinear functions, making it possible to characterize the nonlinearities. A specific measurement system, called a large-signal

network analyzer (LSNA), is usually required to measure and derive this nonlinear behavioral model for the device-under-test (DUT). This theory has not been widely applied in real life thus far due to the limited access to the specialized LSNA systems. Alon [7] provides an interesting time-domain analysis/characterization of the large-signal S -parameters. A modulated signal generator and vector signal analyzer are used to capture the memory effect of the nonlinear devices. However, this technique also requires specific instruments to perform the required measurement, which limits its adoption.

Therefore, one question is asked: is it possible to derive the large-signal behavioral model through generally available measurement systems, e.g., a conventional network analyzer and load–pull measurement system? By looking closely at the LSNA, it is found that the measurement system can be considered as an active harmonic load–pull measurement system [2]. This analogy suggests the possibility to approximately create the large-signal model from a general load–pull measurement dataset.

There are several existing techniques to utilize the load–pull dataset for modeling purposes [8], [9]. Some commercial computer-aided engineering (CAE) software provide the capabilities to read the load–pull data files into the simulator for linear or nonlinear simulation.^{1,2} These techniques create file-based models from the load–pull measurement dataset; the models created can accurately characterize the prescribed load points. The disadvantage of this technique is that it usually involves large file sizes and does not interpolate or extrapolate smoothly. What we will refer to here as the large- S_{21} technique is used in [10] to derive the behavioral model. This technique extends the traditional linear S_{21} to be dependent on the input signal amplitude while keeping other S -parameters constant. A typical swept power S_{21} measurement will give enough information for deriving the large- S_{21} model. Therefore, it can capture the characteristics of small-signal load contours and S_{21} compressions. However, due to the nature of the model derivation (only the gain compression curve at 50 Ω is utilized), it does not take into account and fails to predict the load-related changes in the gain and phase compression curves.

This paper presents a modeling technique that utilizes the load–pull AM–AM and AM–PM measurement datasets to derive the large-signal scattering function model. This is achieved

Manuscript received December 15, 2005; revised May 3, 2006. This work was supported by Modelithics Inc.

The authors are with the Department of Electrical Engineering, University of South Florida, Tampa, FL 33620 USA (e-mail: jliu7@eng.usf.edu).

Digital Object Identifier 10.1109/TMTT.2006.879137

¹Microwave Office, Applied Wave Res. Inc., El Segundo, CA. [Online]. Available: www.microwaveoffice.com

²Advanced Design System (ADS), Agilent Technol., Palo Alto, CA. [Online]. Available: www.agilent.com

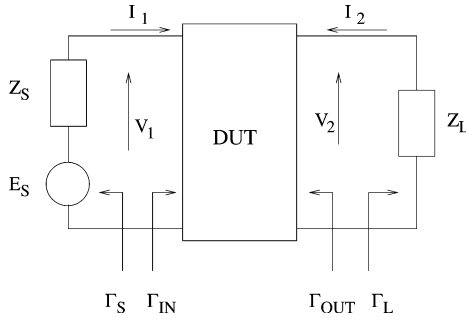


Fig. 1. Diagram of a two-port network with a voltage source of E_s and source impedance of Z_s . The load impedance is Z_L .

through simplifying the original theory and omitting the influence from the harmonics. It is shown that a behavioral model can be created to characterize the load-related gain and phase compression properties accurately.

II. ANALYSIS OF THE BEHAVIORAL MODELING TECHNIQUE

A nonlinear amplifier can be treated as a two-port network shown in Fig. 1. A typical one-tone load-pull measurement gives information about the source impedance (or reflection coefficient Γ_S), load impedances (or reflection coefficient Γ_L), the input power (P_{in}), and the measured delivered power (P_{out}).

To simplify the analysis, suppose the device is unilateral (i.e., $S_{12} = 0$). This constraint can be removed if the input port reflected power is captured in the load-pull measurement. The incident and reflected waveforms at port 1 are calculated as

$$A_1 = \frac{V_1 + I_1 Z_0}{\sqrt{2\text{Re}(Z_0)}} = V_1 M_1 \quad (1)$$

$$B_1 = \frac{V_1 - I_1 Z_0}{\sqrt{2\text{Re}(Z_0)}} = A_1 S_{11} \quad (2)$$

$$M_1 = \frac{Z_0 + Z_{in}}{Z_{in} \sqrt{2\text{Re}(Z_0)}}. \quad (3)$$

By adopting the large-signal scattering function proposed in [4]–[6] and considering only the fundamental tones, we get the incident and reflected waveforms at port 2 in (4) and (5). This model formulation is the result of the linearization around the large-signal operating point of a device and is valid for small A_2 . This extra conjugate term gives us additional flexibility to fit measurement datasets. Notice that, in this simplified model form, the phase normalization introduced in [4] and [5] is neglected. Therefore, this model does not guarantee time invariance; however, as will be demonstrated in the following equation, this deficiency has not led to significant problems, and the consequences will be further explored in the future:

$$B_2 = S_{21}A_1 + S_{22}A_2 + T_{22}A_2^* \quad (4)$$

$$A_2 = B_2\Gamma_L. \quad (5)$$

Combining (4) and (5) gives

$$B_2 = S_{21}A_1 + S_{22}B_2\Gamma_L + T_{22}B_2^*\Gamma_L^*. \quad (6)$$

Equation (6) is an implicit expression for B_2 ; it can be further transformed to an explicit function to simplify the model generation. Assume S_{21} , S_{22} , and T_{22} are represented as

$$S_{21} = c_1 + jc_2$$

$$S_{22} = c_3 + jc_4$$

$$T_{22} = c_5 + jc_6$$

where c_i , ($i = 1, \dots, 6$) are unknowns to be determined.

Suppose $B_2 = B_{2r} + jB_{2i}$ and $A_1 = A_{1r} + jA_{1i}$. B_{2r} and B_{2i} are the real and imaginary parts of B_2 , respectively. A_{1r} and A_{1i} are the real and imaginary parts of A_1 , respectively. Equation (6) can be rewritten as

$$(c_1 + jc_2)A_1 + (k_1 + jk_2)B_2 + (m_1 + jm_2)B_2^* = 0 \quad (7)$$

where

$$k_1 + jk_2 = (c_3 + jc_4)\Gamma_L - 1 \quad (8)$$

$$m_1 + jm_2 = (c_5 + jc_6)\Gamma_L^*. \quad (9)$$

Arrange the real and imaginary parts and we can get

$$\begin{bmatrix} c_1 A_{1r} - c_2 A_{1i} \\ c_1 A_{1i} + c_2 A_{1r} \end{bmatrix} + \begin{bmatrix} k_1 + m_1 & -k_2 + m_2 \\ k_2 + m_2 & k_1 - m_1 \end{bmatrix} \begin{bmatrix} B_{2r} \\ B_{2i} \end{bmatrix} = 0. \quad (10)$$

By solving the linear function (10), the real and imaginary parts of B_2 can be derived as

$$\begin{bmatrix} B_{2r} \\ B_{2i} \end{bmatrix} = \frac{1}{D} \begin{bmatrix} P & Q \\ S & T \end{bmatrix} \begin{bmatrix} A_{1r} \\ A_{1i} \end{bmatrix} \quad (11)$$

where

$$D = k_1^2 - k_2^2 - m_1^2 + m_2^2$$

$$P = (k_1 + k_2 - m_1 - m_2)c_1$$

$$Q = (-k_1 + k_2 + m_1 - m_2)c_2$$

$$S = (k_1 - k_2 + m_1 - m_2)c_1$$

$$T = (k_1 + k_2 + m_1 + m_2)c_2.$$

Obviously, in order to obtain B_{2r} and B_{2i} , the measurements for both the magnitude and phase are required. This is why it is important to obtain the load-pull AM-PM datasets. The load-pull AM-AM measurements provide the optimization criteria for the magnitude, while the load-pull AM-PM measurements set up the rule for the phase optimization.

The magnitude can be derived from the delivered output power. The output power at port 2 is determined by A_2 and B_2 through

$$P_{out} = \frac{1}{2}(|B_2|^2 - |A_2|^2) = \frac{1}{2}|B_2|^2(1 - |\Gamma_L|^2). \quad (12)$$

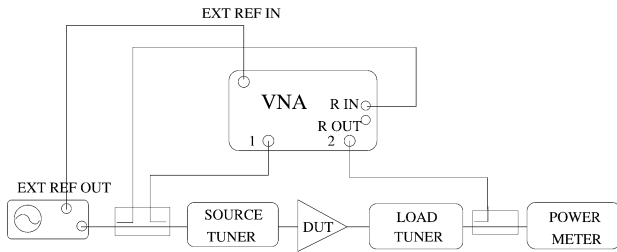


Fig. 2. AM-PM load-pull measurement system diagram.

Since the output power is known through the measurement, the magnitude of B_2 can be expressed as

$$|B_2| = \sqrt{\frac{2P_{\text{out}}}{1 - |\Gamma_L|^2}}. \quad (13)$$

An optimization process can be applied to obtain the six unknown coefficients c_1 – c_6 . The least mean square (LMS) errors for the magnitude and phase can be represented by (14) and (15) as follows:

$$\text{err}_{\text{mag}} = \frac{\sum_n \left((B_{2r}^2 + B_{2i}^2) - \left(\frac{1}{1 - |\Gamma_L|^2} P_{\text{out}} \right) \right)^2}{n} \quad (14)$$

$$\text{err}_{\text{phase}} = \frac{\sum_n \left(\Phi \left(\frac{A_2 + B_2}{A_1 + B_1} \right) - \text{AMPM} \right)^2}{n} \quad (15)$$

where n is the number of load points used in the optimization process. AM-PM is the phase compression data obtained through the load-pull AM-PM measurement. It is the phase difference between the voltages at the input and output ports. The input and output voltages are the sum of the incident and reflected waves at the port, respectively.

To obtain the load-pull AM-PM datasets, an advanced measurement procedure is developed through the integration of the load-pull measurement system and a vector network analyzer (VNA). The setup diagram is shown in Fig. 2. The VNA is used as a vector receiver to obtain the relative AM-PM measurement dataset. The vector receiver captures the incoming signals and stores the corresponding complex values as an array in the instrument memory. The AM-PM curve is generated by normalizing the phases of these complex values against the phase of the first complex value in the array.

The analysis given above has been implemented in a MATLAB program.³ Fig. 3 demonstrates the procedure to generate the behavioral model based on the load-pull datasets. The two error functions are normalized, respectively, and formulated into a weighted function in the MATLAB program. Notice that the load-pull datasets can come from either the measurements or from simulations, depending on the applications of this modeling technique.

³The MathWorks Inc., Natick, MA. [Online]. Available: www.mathworks.com

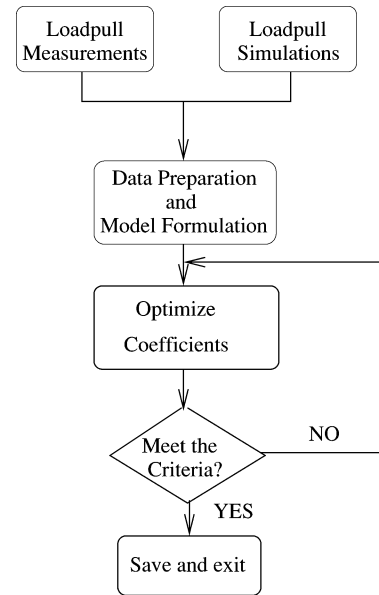


Fig. 3. Flowchart of the MATLAB program created for the behavioral model optimization based on the load-pull AM-AM and AM-PM datasets.

III. EXAMPLE MODEL OF A PA SAMPLE

To illustrate this modeling technique, an example model is created based on the measurement datasets for a ISL3984 PA sample. This sample amplifier was characterized at 2.45 GHz. Load-pull gain and phase compression measurements were performed. Two-tone load-pull measurements were performed as well. The MATLAB modeling program was used to process the measurement data files and generate the model coefficients through the unconstrained nonlinear optimization procedure. The measurement condition is summarized as follows:

- frequency: 2.45 GHz;
- input power: -22 – 3.5 dBm;
- two-tone frequency spacing: 100 kHz;
- bias: 3.3 V.

The model was implemented in ADS 2004A using the frequency-domain defined (FDD) device. The advantage of using this device is that it provides the ability to define the behavior of individual frequency components separately. Notice that although only the ADS implementation of the behavioral model is shown in this paper, this technique is general enough to be implemented in other CAE software. Fig. 4 compares the measured and simulated gain and phase compression performance of this PA at $50\text{-}\Omega$ condition. The model predicts the compression property correctly.

Figs. 5 and 6 illustrate the optimized large-signal S_{22} and T_{22} coefficients versus input power levels. As you can see, the S_{22} demonstrates strong compression at higher input power levels. The T_{22} coefficient presents significant contributions at high input power. Therefore, it is important to characterize these effects instead of treating them as linear/constant.

Fig. 7 shows the simulated output power contours compared with the measured result. The input power is at -20 dBm. Good agreement can be observed in this figure. In fact, the large-signal model reduces to a small-signal S -parameter model when the input signal is low enough. The variation of the output power

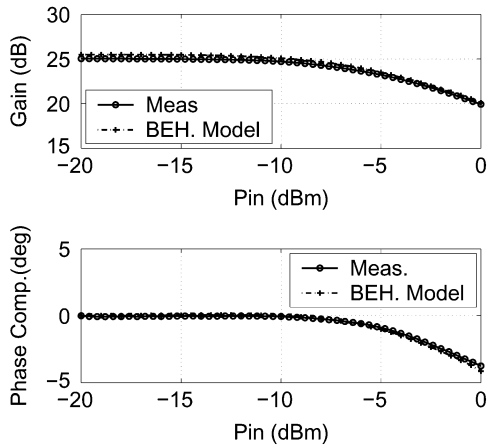


Fig. 4. Comparison of the measured and simulated gain and phase compression at 50 Ω .

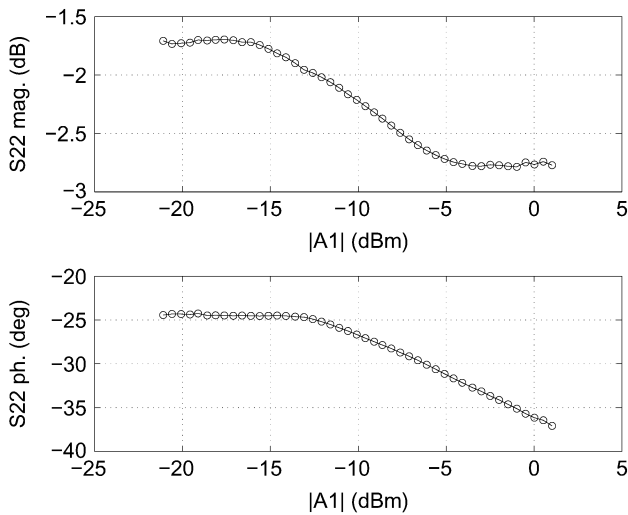


Fig. 5. Optimized S_{22} versus P_{in} .

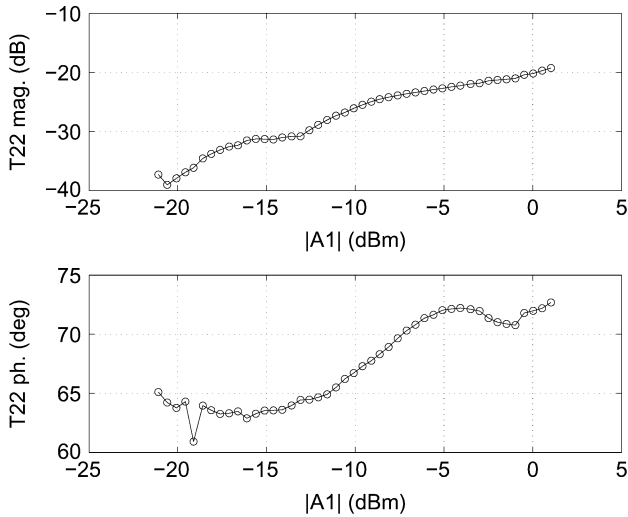


Fig. 6. Optimized T_{22} versus P_{in} .

with respect to the load can be characterized through the small-signal S -parameter. Detailed analysis can be found in [11].

Six load impedances are chosen as examples to test the large-signal model. The reflection coefficients of the six example loads are listed in Table I and plotted in a Smith chart, as

Pout comparison (P_{in} at -20 dBm): behavioral model vs. measurement

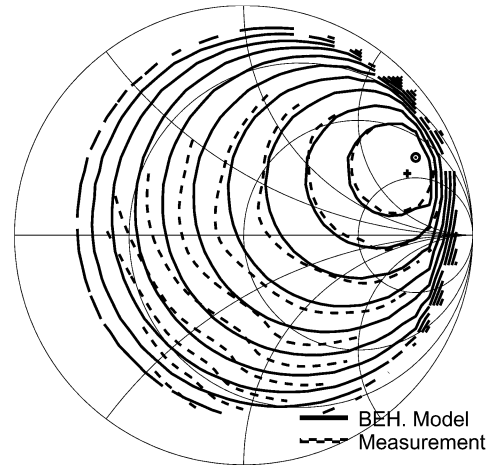


Fig. 7. Comparison of the simulated output power contour with the measured dataset.

TABLE I
LIST OF THE SIX EXAMPLE LOAD REFLECTION COEFFICIENTS USED TO TEST THE PA MODEL

(a)	$0.62561+j*0.39360$	(b)	$-0.36966+j*0.09652$
(c)	$0.19215+j*0.33529$	(d)	$0.87741+j*0.07210$
(e)	$0.61180+j*0.627895$	(f)	$0.52078-j*0.53337$

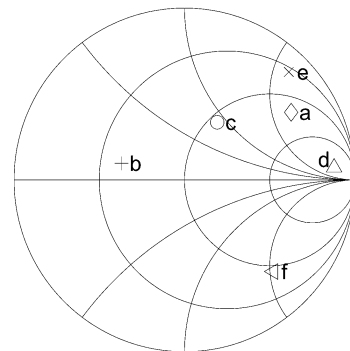


Fig. 8. Illustration of the six load impedance examples on the Smith chart.

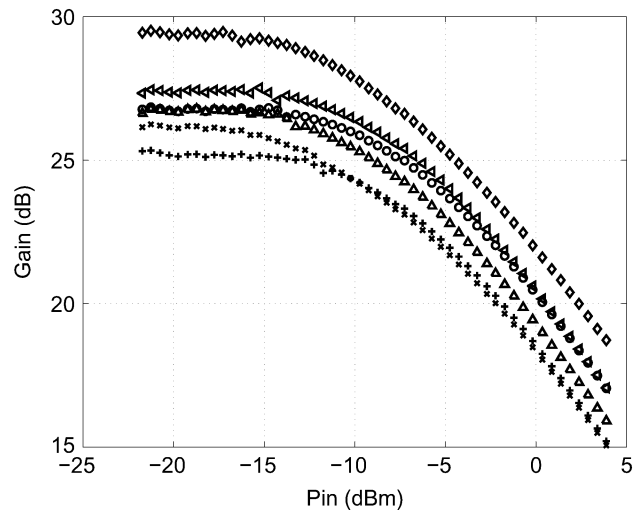


Fig. 9. Simulated fundamental tone at six loads are plotted. The markers of the curve are consistent with Fig. 8.

shown in Fig. 8. The load examples are chosen to spread over the Smith chart.

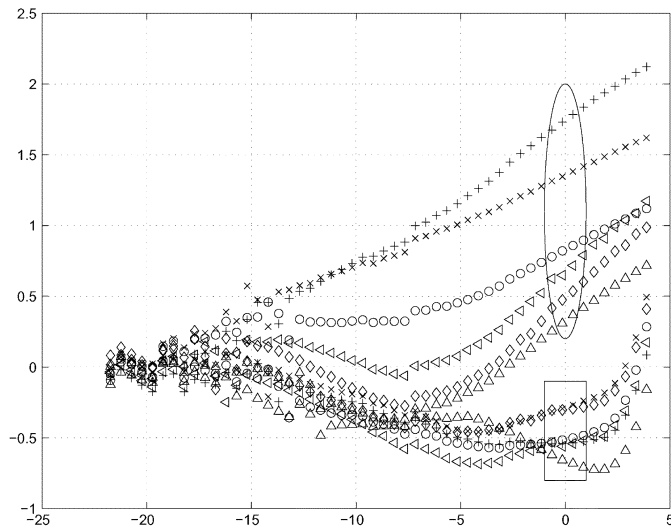


Fig. 10. Errors of the simulated fundamental tone at six loads are plotted. The black curves (enclosed by the rectangle) represent the errors associated with the newly developed model; the gray curves (enclosed by the ellipse) represent the errors associated with the large- S_{21} model. The new model presents better performance, compared with the large- S_{21} model.

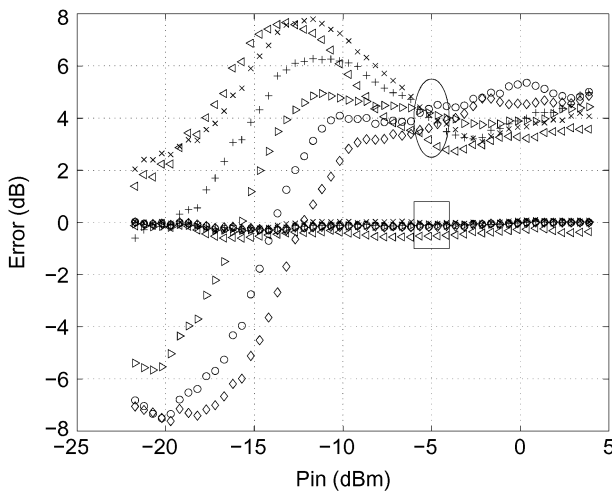


Fig. 11. Errors of the simulated IM3 product at six loads are plotted. The black curves (enclosed by the rectangle) represent the errors associated with the newly developed model; the gray curves (enclosed by the ellipse) represent the errors associated with the large- S_{21} model. The new model presents better performance compared with the large- S_{21} model.

Fig. 9 shows the gain compression curves measured at the six loads. The markers of the curve are consistent with Fig. 8. As one can see, the compression rates of this device are different at different load points. Therefore, it is important to consider this effect when modeling a device. However, as mentioned in Section I, the large- S_{21} modeling technique only considers the nonlinear effect of S_{21} based on the gain compression measurement done at $50\ \Omega$. This limitation makes the large- S_{21} modeling technique inaccurate when the load points are significantly deviated from $50\ \Omega$.

As can be seen in Fig. 10, the proposed model presents a much better performance in predicting the gain compression effects of the device at different loads than the large- S_{21} model does.

Since only the fundamental tone is considered and characterized during the model generation, its capability to predict

the intermodulation products (which involves higher order harmonics) is limited. Therefore, to solve this issue, a file-based model is implemented for prediction of the third-order intermodulation (IM3) products. A contour interpolation algorithm is utilized during the generation of the data file. Fig. 11 illustrates the errors in the simulated IM3 at different loads. The new model has significantly better performance compared with the large- S_{21} model.

IV. CONCLUSION

A behavioral modeling technique has been presented that is directly derived on the load-pull gain and phase compression measurements. Simplified from the large-signal scattering function theory, the model formulation neglects the harmonic terms and phase normalization. An example model for a PA sample is given to demonstrate the possibility to generate the large-signal scattering function model using traditional load-pull measurement systems and exploiting advanced measurement procedures. Good agreement is observed between the simulated results and measurement datasets. More study is required in future research to study the consequences of neglecting the phase normalization.

ACKNOWLEDGMENT

The authors thank J. Verspecht, Jan Verspecht bvba, Steenhuffel, Belgium, for his valuable suggestions and insights.

REFERENCES

- [1] J. Verspecht, M. V. Bossche, and F. Verbeyst, "Characterizing components under large signal excitation: Defining sensible 'large signal S -parameters'," in *49th ARFTG Conf. Dig.*, Jun. 1997, pp. 109–117.
- [2] J. Verspecht and P. V. Esch, "Accurately characterizing hard nonlinear behavior of microwave components with the nonlinear network measurement system: Introducing 'nonlinear scattering functions'," in *Proc. 5th Int. Integr. Nonlinear Microw. Millimeterwave Circuits Workshop*, Oct. 1998, pp. 17–26.
- [3] J. Verspecht, "Large-signal network analysis—Going beyond s -parameters," presented at the 52nd ARFTG Conf., Dec. 2003, Short course notes.
- [4] J. Verspecht, D. Root, J. Wood, and A. Cognata, "Broad-band, multi-harmonic frequency domain behavioral models from automated large-signal vectorial network measurements," in *IEEE MTT-S Int. Microw. Symp. Dig.*, Jun. 2005, 4 pp.
- [5] D. E. Root, J. Verspecht, D. Sharrit, J. Wood, and A. Cognata, "Broad-band poly-harmonic distortion (PHD) behavioral models from fast automated simulations and large-signal vectorial network measurements," *IEEE Trans. Microw. Theory Tech.*, vol. 53, no. 11, pp. 3656–3664, Nov. 2005.
- [6] J. Verspecht, D. F. Williams, D. Schreurs, K. A. Remley, and M. D. McKinley, "Linearization of large-signal scattering functions," *IEEE Trans. Microw. Theory Tech.*, vol. 53, no. 4, pp. 1369–1376, Apr. 2005.
- [7] Z. Alon, "Extraction and application of behavioral models in power amplifier simulation," Master's thesis, Dept. Elect. Comput. Eng., Univ. California at Santa Barbara, Santa Barbara, CA, 2003.
- [8] J. Olah and S. Gupta, "Power amplifier design using measured load-pull data," in *Microw. Eng. Europe*, Aug. 2003, pp. 23–30.
- [9] R. L. Carlson, "Meld load-pull test with EDA tools," *Microw. RF*, Apr. 2003 [Online]. Available: <http://www.mwrf.com/Articles/ArticleID/5448/5448.html>
- [10] W. Clausen, J. Capwell, L. Dunleavy, T. Weller, J. Verspecht, J. Liu, and H. Arslan, "Black-box modeling of RFIC amplifiers for linear and non-linear simulations," *Microw. Product Dig.*, p. 34, Oct. 2004.
- [11] G. Gonzalez, *Microwave Transistor Amplifiers: Analysis and Design*, 2nd ed. Englewood Cliffs, NJ: Prentice-Hall, 1996.



Jiang Liu received the M.S.E.E. and Ph.D. degrees from University of South Florida, Tampa, in 2002 and 2005, respectively.

He is currently a consultant providing services in the area of nonlinear modeling and customized measurement procedure developments. His main research interests are in advanced RF and microwave measurement procedure developments and behavioral modeling techniques for nonlinear RF devices or components.



Lawrence P. Dunleavy (S'80–M'82–SM'96) received the B.S.E.E. degree from Michigan Technological University, Houghton, in 1982, and the M.S.E.E. and Ph.D. degrees from The University of Michigan at Ann Arbor, in 1984 and 1988, respectively.

Along with four faculty colleagues, he established the Center for Center for Wireless and Microwave Information Systems, University of South Florida, Tampa. In 2001, he co-founded Modelithics Inc., a USF spinoff company to provide a practical commercial outlet for developed modeling solutions and microwave measurement

services. He has been involved in industry for E-Systems (1982–1983) and Hughes Aircraft Company (1984–1990), and was a Howard Hughes Doctoral Fellow (1984–1988). In 1990, he joined the Department of Electrical Engineering, University of South Florida, where he is currently a Professor. He guides a team of graduate students in various research projects related to microwave and millimeter-wave device, circuit, and system characterization and modeling. From 1997 to 1998, he spent a sabbatical year with the Noise Metrology Laboratory, National Institute of Standards and Technology (NIST), Boulder, CO. He has authored or coauthored over 75 technical papers.

Dr. Dunleavy is very active in the IEEE Microwave Theory and Techniques Society (IEEE MTT-S) and the Automatic RF Techniques Group (ARFTG).



Huseyin Arslan (S'95–M'98–SM'04) received the Ph.D. degree from Southern Methodist University (SMU), Dallas, TX, in 1998.

From January 1998 to August 2002, he was with the Research Group, Ericsson Inc., Research Triangle Park, NC, where he was involved with several project related to second-generation (2G) and third-generation (3G) wireless cellular communication systems. Since August 2002, he has been with the Department of Electrical Engineering, University of South Florida, Tampa. He was also a Visiting Professor (Summer 2005) and has been a Part-Time Consultant (since August 2005) with the Anritsu Company, Morgan Hill, CA. His research interests are related to advanced signal-processing techniques at the physical layer with cross-layer design for networking adaptivity and quality of service (QoS) control. More specifically, he is interested in signal-processing techniques for wireless communication systems including modulation and coding, interference cancellation and multiuser signal detection, channel estimation and tracking, equalization, soft information generation, adaptive receiver, transmission technologies, etc. He is interested in many forms of wireless technologies including cellular, wireless personal area networks (PANs)/local area networks (LANs)/metropolitan area networks (MANs), fixed wireless access, and specialized wireless data networks like wireless sensors networks and wireless telemetry. His current research interests are ultra-wideband (UWB), orthogonal frequency-division multiplexing (OFDM)-based wireless technologies with emphasis on WIMAX, and cognitive and software-defined radio. He is an Editorial Board member for the *Wireless Communication and Mobile Computing Journal*.

Dr. Arslan has served as a Technical Program Committee member, session and symposium organizer for several IEEE conferences. He was Technical Program co-chair for the 2004 IEEE Wireless and Microwave Conference.